AFRL-AFOSR-VA-TR-2016-0195

Fundamental Structure of High-Speed Reacting Flows: Supersonic Combustion and Detonation

Kenneth Yu
MARYLAND UNIV COLLEGE PARK

05/05/2016
Final Report

Air Force Research Laboratory
AF Office Of Scientific Research (AFOSR)/ RTA1
Arlington, Virginia 22203
Air Force Materiel Command

REPORT DOCUMENTATION PAGE

Form Approved
OMB No. 0704-0188

PLEASE DO NOT RETURN YOUR FORM TO THE ABOVE ORGANIZATION.

1. REPORT DATE *(DD-MM-YYYY)*	2. REPORT TYPE	3. DATES COVERED *(From - To)*
30-04-2016	FINAL REPORT	MARCH 2013 - MARCH 2016

4. TITLE AND SUBTITLE
FUNDAMENTAL STRUCTURE OF HIGH-SPEED REACTING FLOWS: SUPERSONIC COMBUSTION AND DETONATION

5a. CONTRACT NUMBER

5b. GRANT NUMBER
FA9550-13-1-0080

5c. PROGRAM ELEMENT NUMBER

6. AUTHOR(S)
KENNETH H. YU
JASON BURR
ROBERT FIEVISOHN

5d. PROJECT NUMBER

5e. TASK NUMBER

5f. WORK UNIT NUMBER

7. PERFORMING ORGANIZATION NAME(S) AND ADDRESS(ES)
UNIVERSITY OF MARYLAND
DEPARTMENT OF AEROSPACE ENGINEERING
COLLEGE PARK, MD 20742

8. PERFORMING ORGANIZATION REPORT NUMBER

9. SPONSORING/MONITORING AGENCY NAME(S) AND ADDRESS(ES)
AIR FORCE OFFICE OF SCIENTIFIC RESEARCH
875 NORTH RANDOLPH ST
ARLINGTON, VA 22203

10. SPONSOR/MONITOR'S ACRONYM(S)

11. SPONSOR/MONITOR'S REPORT NUMBER(S)

12. DISTRIBUTION/AVAILABILITY STATEMENT
DISTRIBUTION A

13. SUPPLEMENTARY NOTES

14. ABSTRACT
An experimental investigation on detonation wave propagating across a row of reactant jets in a narrow channel has been performed. The principal objective of the research was to gain better understanding of the fundamental flow structure in a rotating detonation engine (RDE). A linear channel simulating an unwrapped RDE annulus was used for the investigation with an array of fifteen injectors lining the inlet plane. The resulting flow structure caused by a detonation wave propagating across the array of reactant jets was examined as a function of reactant composition and flow rates. This setup served as the baseline configuration for investigating the RDE flowfield with the curvature effect. The overall research effort comprised of the following technical elements: (1) blast wave propagation under partial confinement, (2) detonation wave experiments in a transvers flow channel, (3) modeling of detonation wave in transvers flow using a method of characteristics approach. The specific objectives and results of the research of each of these program elements are summarized in this report.

15. SUBJECT TERMS
DETONATION WAVE PROPAGATION IN LINEAR CHANNEL WITH TRANSVERS JETS

16. SECURITY CLASSIFICATION OF:			17. LIMITATION OF ABSTRACT	18. NUMBER OF PAGES	19a. NAME OF RESPONSIBLE PERSON
a. REPORT	b. ABSTRACT	c. THIS PAGE			KENNETH YU
U	U	U	UU		19b. TELEPHONE NUMBER *(Include area code)* (301)405-1333

Standard Form 298 (Rev. 8/98)
Prescribed by ANSI Std. Z39.18
Adobe Professional 7.0

INSTRUCTIONS FOR COMPLETING SF 298

1. REPORT DATE. Full publication date, including day, month, if available. Must cite at least the year and be Year 2000 compliant, e.g. 30-06-1998; xx-06-1998; xx-xx-1998.

2. REPORT TYPE. State the type of report, such as final, technical, interim, memorandum, master's thesis, progress, quarterly, research, special, group study, etc.

3. DATES COVERED. Indicate the time during which the work was performed and the report was written, e.g., Jun 1997 - Jun 1998; 1-10 Jun 1996; May - Nov 1998; Nov 1998.

4. TITLE. Enter title and subtitle with volume number and part number, if applicable. On classified documents, enter the title classification in parentheses.

5a. CONTRACT NUMBER. Enter all contract numbers as they appear in the report, e.g. F33615-86-C-5169.

5b. GRANT NUMBER. Enter all grant numbers as they appear in the report, e.g. AFOSR-82-1234.

5c. PROGRAM ELEMENT NUMBER. Enter all program element numbers as they appear in the report, e.g. 61101A.

5d. PROJECT NUMBER. Enter all project numbers as they appear in the report, e.g. 1F665702D1257; ILIR.

5e. TASK NUMBER. Enter all task numbers as they appear in the report, e.g. 05; RF0330201; T4112.

5f. WORK UNIT NUMBER. Enter all work unit numbers as they appear in the report, e.g. 001; AFAPL30480105.

6. AUTHOR(S). Enter name(s) of person(s) responsible for writing the report, performing the research, or credited with the content of the report. The form of entry is the last name, first name, middle initial, and additional qualifiers separated by commas, e.g. Smith, Richard, J, Jr.

7. PERFORMING ORGANIZATION NAME(S) AND ADDRESS(ES). Self-explanatory.

8. PERFORMING ORGANIZATION REPORT NUMBER. Enter all unique alphanumeric report numbers assigned by the performing organization, e.g. BRL-1234; AFWL-TR-85-4017-Vol-21-PT-2.

9. SPONSORING/MONITORING AGENCY NAME(S) AND ADDRESS(ES). Enter the name and address of the organization(s) financially responsible for and monitoring the work.

10. SPONSOR/MONITOR'S ACRONYM(S). Enter, if available, e.g. BRL, ARDEC, NADC.

11. SPONSOR/MONITOR'S REPORT NUMBER(S). Enter report number as assigned by the sponsoring/ monitoring agency, if available, e.g. BRL-TR-829; -215.

12. DISTRIBUTION/AVAILABILITY STATEMENT. Use agency-mandated availability statements to indicate the public availability or distribution limitations of the report. If additional limitations/ restrictions or special markings are indicated, follow agency authorization procedures, e.g. RD/FRD, PROPIN, ITAR, etc. Include copyright information.

13. SUPPLEMENTARY NOTES. Enter information not included elsewhere such as: prepared in cooperation with; translation of; report supersedes; old edition number, etc.

14. ABSTRACT. A brief (approximately 200 words) factual summary of the most significant information.

15. SUBJECT TERMS. Key words or phrases identifying major concepts in the report.

16. SECURITY CLASSIFICATION. Enter security classification in accordance with security classification regulations, e.g. U, C, S, etc. If this form contains classified information, stamp classification level on the top and bottom of this page.

17. LIMITATION OF ABSTRACT. This block must be completed to assign a distribution limitation to the abstract. Enter UU (Unclassified Unlimited) or SAR (Same as Report). An entry in this block is necessary if the abstract is to be limited.

Final Report

on

Fundamental Structure of High-Speed Reacting Flows:

Supersonic Combustion and Detonation

Grant Number: FA9550-13-1-0080

Prepared for

AIR FORCE OFFICE OF SCIENTIFIC RESEARCH

For the Period

27 March 2013 to 31 March 2016

Submitted by:

Ken H. Yu
Department of Aerospace Engineering
University of Maryland
College Park, MD 20742
yu@umd.edu
(301) 405-1333

TABLE OF CONTENTS

1.0 SUMMARY

An experimental investigation on detonation wave propagating across a row of reactant jets in a narrow channel has been performed. The principal objective of the research was to gain better understanding of the fundamental flow structure in a rotating detonation engine (RDE). A linear channel simulating an unwrapped RDE annulus was used for the investigation with an array of 15 injectors lining the inlet plane. The resulting flow structure caused by a detonation wave propagating across the array of reactant jets was examined as a function of reactant composition and flow rates. This setup served as the baseline configuration for investigating the RDE flow field without the curvature effect. The overall research effort comprised of the following technical elements: (1) blast wave propagation under partial confinement, (2) detonation wave experiments in a transverse flow channel, (3) modeling of detonation wave in transverse flow using a method of characteristics approach. The specific objectives and results of the research of each of these program elements are summarized in this report.

2.0 INTRODUCTION

2.1 Background

Early investigators studying tangential mode combustion instabilities reported observations of rotating detonation-like waves in liquid rocket engines, studied the concept of rotating detonation rocket engine in both gaseous and two-phase propellants. Recently, there have been renewed interests on rotating detonation engine (RDE) concept driven by potential benefits on thermodynamic efficiency of detonation cycle over constant pressure engines. There are a number of on-going investigations studying various aspects of RDE, from understanding basic physics to integrating RDE to aerospace platforms. These studies have followed the recent progress in the pulsed detonation engine (PDE) studies, but with some notable differences in the research approach and the amount of previous knowledge in the relevant detonation structure.

For instance, in studying PDE phenomena, simple confined tube geometry of this configuration made it possible to apply one-dimensional approximation and simplified analysis, even though both turbulence features and detonation phenomenon are inherently three-dimensional. Also, the results from early experimental studies in the 1960s showing detonation structure clearly in a duct, are still relevant for many aspects of PDE studies of today. Therefore, it was possible to focus the initial efforts of PDE investigation more on the development and system issues, such as fuels, ignition, frequencies, injection timing, mixing, controlling, etc.

In studying rotating detonation engines, however, it is no longer viable to use results from any one-dimensional approximation for detonation wave, since it propagates in an orthogonal direction to the flow. Even the simplest framework would require a two-dimensional geometry, which makes understanding from the simplified detonation model less relevant. Any prediction of detailed detonation wave structure in RDE is very challenging. From the research community's perspective, we need fundamental studies that can isolate the relevant flow and chemistry features in RDE and that can thoroughly investigate those features in more detail.

While there are numerous CFD studies simulating the three-dimensional detonation structure in RDE models, there has been very little experimental data available for comparison or for guidance of future simulation results.

The principal objective of this research is to gain a more fundamental understanding of the detailed flow structure in a rotating detonation engine flow field by recreating experimentally the transverse or tangential propagation of the detonation wave in a straight channel that simulates the annular passage in an RDE, for example one with an infinite radius. This will allow us to investigate key features of the transverse detonation wave structure thoroughly, with exceptional details as those provided by those early studies of detonation in tube. The specific objective is to obtain detailed information on fundamental detonation structure representative of an RDE configuration. At first, we attempt to simplify the physics contained in the flow problem and lessen the experimental complications by not considering the curvature effect and the associated centripetal acceleration in an annulus of RDE. Studying transverse detonation in a straight channel instead of an annulus would provide a tremendous advantage in our ability to obtain high-quality flow visualization, with presumably negligible effect on the essence of the detonation structure.

2.2 Approach

Simple canonical configurations for studying rotating detonation engine flow structure are shown in Fig. 2.1. The experimental approach is to simplify a rotating detonation engine flowfield by considering detonation waves propagating across transvers flow of reactant jets, similar to that shown in Fig. 2.1(a). For analytical approach, even a simpler configuration shown in Fig. 2.1(b) is utilized.

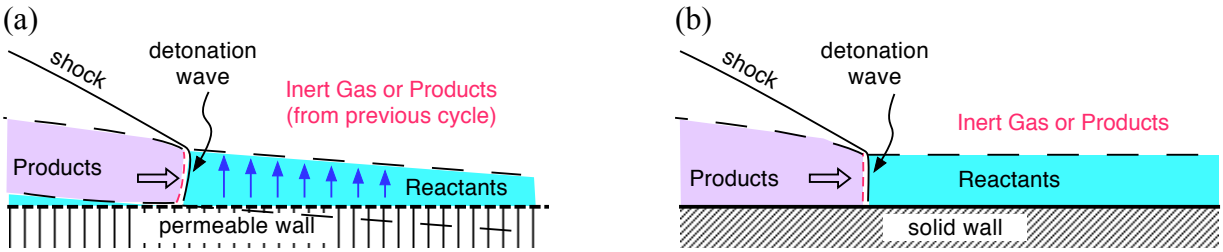

Figure 2.1. Simplified canonical configurations for RDE flow structure study
(a) detonation wave in transverse flow, (b) detonation wave in free boundary

One revolution of an RDE cycle is simulated in an experimental setup analogous to an unwrapped RDE channel that stretches linearly. A straight channel is much more advantageous for high-quality flow visualization and diagnostics. This approach is illustrated in Fig. 2.2. A straight channel simulating a linear RDE model provides a good optical access for detailed investigation of detonation structure. The detonation wave is initiated using a single pulse detonation tube.

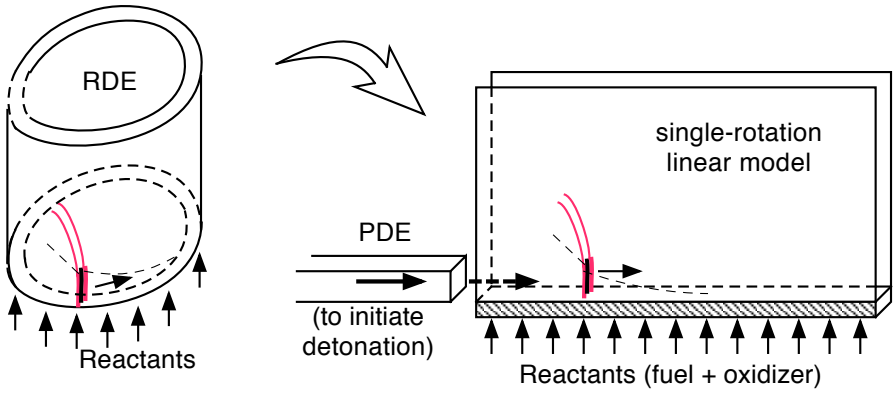

Figure 2.2. Illustration of Cartesian coordinate simulation of RDE wave structure using a PDE wave initiation and a row of linearly arranged injectors.

For companion analytical study, the detonation wave bounded between free stream on one side and solid wall on the other was modeled using shock-expansion theory and two-dimensional method of characteristics. This was an extension of similar approach adopted by Sommers & Morrison [1] and Sichel & Foster [2], but focused specifically on RDE applications and performance analyses. Figure 2.3 illustrates a geometric representation of the problem in a wave-stationary frame of reference. In this configuration, the flow direction is reversed to have the reactants flowing from left to right while the detonation wave remains stationary.

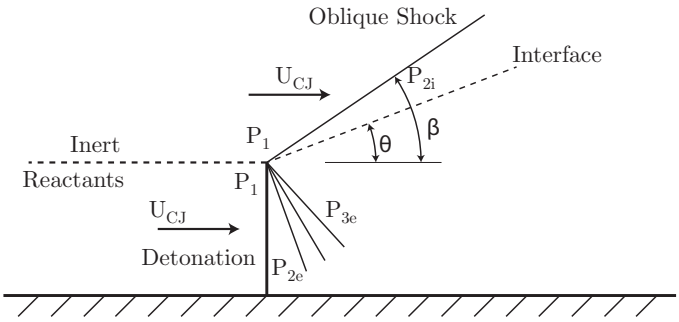

Figure 2.3. A model flow configuration simplified for RDE analysis.

3.0 BLAST WAVE PROPAGATION UNDER PARTIAL OR NO CONFINEMENT

3.1 Objectives

The goal is to better understand the fundamental structure associated with RDE operation by conducting experiments in a linear channel analogous to an unwrapped RDE channel. Toward this goal, the specific objectives of this particular task are (1) to establish the kinematic behavior of blast waves propagating inside an RDE channel, (2) to compare the blast wave behavior under partial confinement conditions, and (3) to study dynamics interaction between blast waves and transverse flow jets. These conditions simulate the various flow-field conditions that may be encountered during RDE operation. Some examples of such conditions include the flow field (i) just prior to a detonation wave initiation, (ii) when a detonation wave passes over a non-detonable medium such as the products, or (iii) just after an extinction event, etc.

3.2 Experimental Setup

A schematic of the PDE is shown with a cross-sectional view in Fig. 3.1. A detonation wave is produced with a hydrogen-oxygen mixture injected near the stoichiometric ratio. The tube is 16.4 inch long and its inner diameter is 0.43 inch. During the initial set of runs, the measured wave speed was 2320 ± 140 m/s, which is about 82% of the

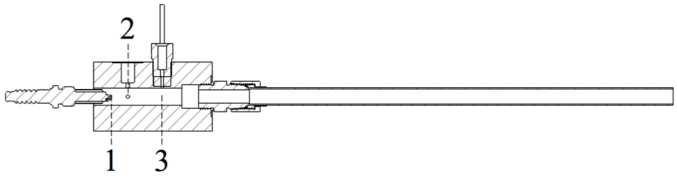

Figure 3.1. Cross-section view of the PDE. Positions 1, 2, and 3 correspond to the spark ignition source, injector location, and a dynamic pressure transducer port, respectively.

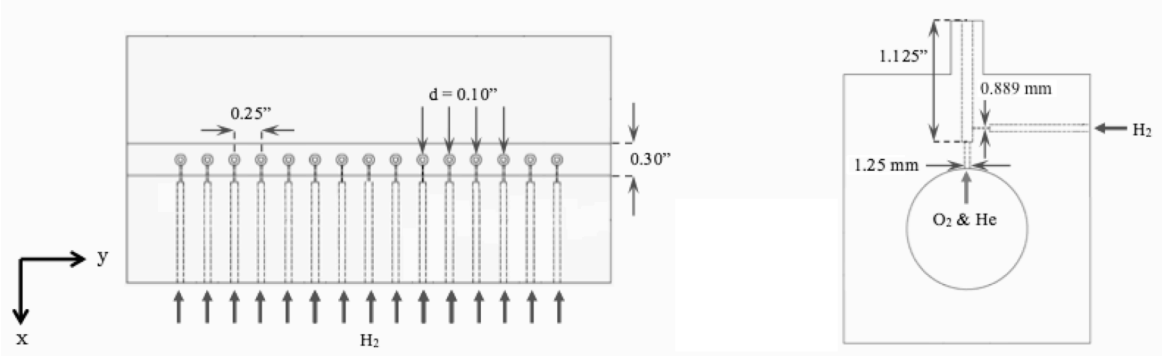

Figure 3.2. Linear Model Detonation Engine (LMDE) injector array. The detonation wave propagates in the y-direction, while the transvers reactants flow is discharged in the z-direction.

Chapman-Jouguet (CJ) speed for the stoichiometric mixture. As the detonation wave exits the PDE tube into the non-reactive surrounding, a decaying blast wave is formed. If more reactants are injected into the wave path, it may be possible to reinitiate the detonation wave under certain conditions.

Downstream of the PDE exit, a series of transvers jets are injected through the Linear Model Detonation Engine (LMDE), shown in Fig. 3.2. The LMDE is a two-dimensional representation of an RDE with the injectors aligned linearly along a straight channel rather than in an annular

channel. Under certain conditions, injection of reactants along the channel can sustain the transversely propagating detonation wave.

In particular the LMDE combines attributes of the Air Force Research Lab's (AFRL) 6-inch RDE [3] and the Naval Research Lab's (NRL) premixed microinjection system [4]. Fifteen recessed tubes with 1.125-inch in length and 0.10-inch diameter are used to establish premixed jets of hydrogen, oxygen, and inert gas mixtures. They are injected in the z-direction, transversely across the wave propagation in the y-direction. Flow conditions for the LMDE are summarized in Table 3.1.

Table 3.1: LMDE Flow Conditions

Continuous Flow Conditions	Symbol	Value
Atmospheric Temperature	T_{air}	298 K
Atmospheric Pressure	P_{air}	14.7 psi
Hydrogen Flow Rate	$\dot{m}_{H2}$	0.290 g/s
Oxygen Flow Rate	$\dot{m}_{O2}$	2.29 g/s
Helium Flow Rate	$\dot{m}_{He}$	0.858 g/s
Hydrogen-Oxygen Equivalence Ratio	ϕ_{LMDE}	1.0
Helium Dilution (Total Molar)	D_{He}	50%

To form a partially open geometry for the blast wave, a flat plate is positioned at the base of the LMDE injectors to form a flanged injection setup and the exit of the PDE tube rests at one end of the LMDE, as shown in Fig. 3.3. The resulting wave propagates into an open hemisphere, with only the bottom wall providing partial confinement for the wave reflection. In this configuration the LMDE behaves as two-dimensional RDE with the combustor tube removed.

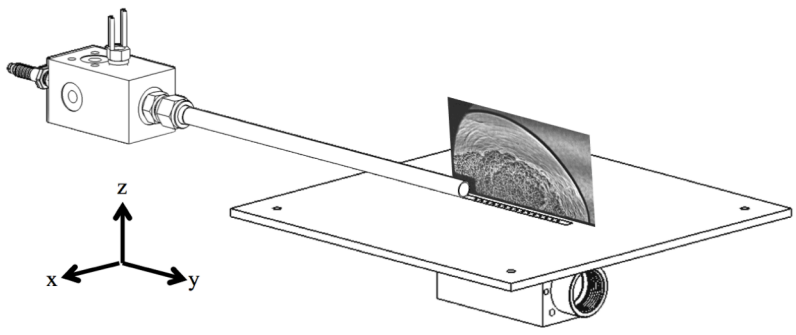

Figure 3.3. Dimetric projection of the setup, showing the PDE and LMDE assembly with a flange plate. Blast waves and transvers jets propagate in the positive y- and z-direction, respectively. Shadowgraph image illustrates a view in the y-z plane

Both schlieren visualization and shadowgraph technique were used to obtain flow structure images of the PDE-generated blast wave interacting with the LMDE injected transvers flow in the y-z plane. Images were acquired in single-shot mode for each run. Thus, each image represents a flow field from a different run. A computer-controlled timing sequencer is employed

to ensure proper synchronization between PDE operation and LMDE injectant height and help achieve run-to-run reproducibility.

Kistler dynamic pressure transducers were used in conjunction with a National Instruments cDAQ-9188. Three Kistlers positioned just after the exit of the PDE tube, spaced along the y-axis and next to the cross-flow jet, were used to measure average blast wave speeds. The Kistler sensors have a range of ±100 psi and were sampled at 750 kHz. The measured values were sent via a TCP/IP connection to a desktop computer operating a LabView control panel. This interface subsequently wrote the data to a text file for use by post-processing software.

3.3 Research Results (by Jason Burr, MS Degree Candidate)

Blast Wave Propagation With No Confinement and No Transverse flow

The blast wave structure was visualized without the transvers flow present to establish a baseline for subsequent comparison. Minimizing PDE fill time mitigated reactants spillage in the y-direction along the top of the LMDE. Image acquisition was controlled relative to the PDE ignition trigger.

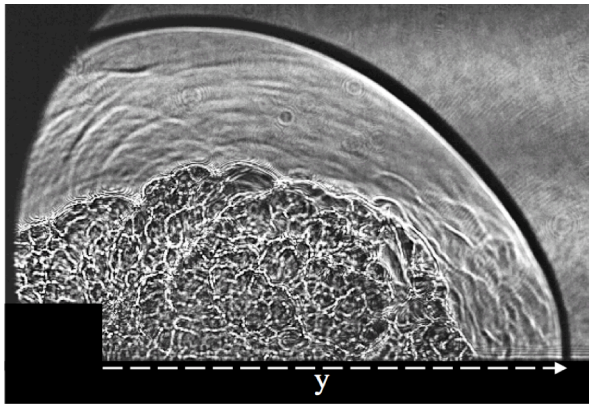

Figure 3.4. Blast wave traversing the LMDE surface in the absence of transverse flow.

Figure 3.4 shows a typical shadowgraph image of a blast wave (y-z plane) without reactants flow. The largely hemispherical blast wave is characterized by a sharp shock front that precedes the region of combustion within the blast wave. This combustion region produces pressure waves that catch up to the shock and reinforce it. These pressure waves appear as ripples in the region between the shock front and the combustion region.

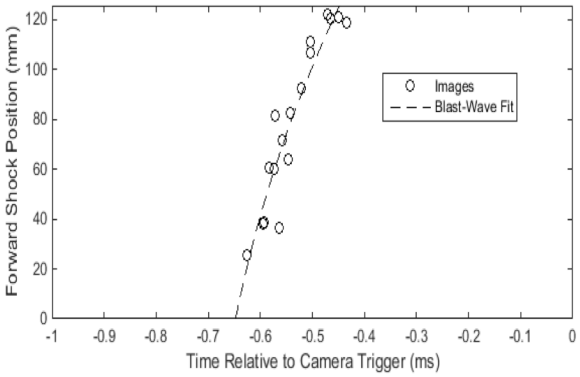

Figure 3.5. Forward position of the blast wave correlated with the reference time.

From these shadowgraph images the position of the forward shock in the y-direction was measured relative to the exit of the PDE. Figure 3.5 compares the forward position of the blast wave to the reference time when each image was acquired. Image acquisition occurs in a 1-ms window prior to the camera trigger with the exact time determined by a synch signal independent of the controller.

A blast wave trajectory as a function of time from a point source was estimated using the following form [5]:

$$y(t) = A\left(t - t_0\right)^{2/5} - y_0$$

where t_0 and y_0 represented initial time and location where the detonation wave from the PDE first disintegrated into a blast wave and A, an energy correlation parameter. Appropriate empirical fitting of the parameter yielded the curve in Figure 3.5. The average blast wave speed across the LDME surface was about 630 m/s in the absence of any cross-flow. Slight variations in the deflagration-to-detonation transition location within the PDE tube as well as the initial location of the detonation wave decoupling after exit would contribute to uncertainty in the precise timing correlation.

Additional velocity estimates were made using dynamic pressure transducer measurements taken at positions of y=0.5 inch, 2.0 inch, and 3.5 inch along the y-axis relative to the exit of the PDE tube. The shock front produced a sharp rise in the dynamic pressure signal, and the average speed between two adjacent sensors was calculated using the pressure signals.

For the baseline configuration without transvers flow, the average shock speed was 870 ± 120 m/s for 12.7mm ≤ y ≤ 50.8 mm and 570 ± 35 m/s for 50.8mm ≤ y ≤ 88.9 mm. Using the parameters used in Fig. 3.5, the average velocity in these ranges is estimated to be 792 m/s and 606 m/s, respectively, both within the standard deviations of the measurements.

Blast Wave Propagation With No Confinement But With Transvers Flow

A consistent cross-flow was established by calibrating the height of the gases in time relative to the controller commands, and then staggering the triggering of the gases such that each species – hydrogen, helium, and oxygen – independently reached the desired height when the blast wave traversed the LMDE in the positive y direction. The transvers jet velocity in all test cases was relatively small – on the order of tens of meters per second – relative to the detonation wave speed within the PDE, 2320 m/s.

Two different transvers flow mixtures were considered – one comprised entirely of a stoichiometric hydrogen-oxygen mixture, and another stoichiometric hydrogen-oxygen mixture that includes 50% helium in molar composition. Transvers flow heights were normalized by the characteristic detonation cell sizes (λ) for the mixtures – for the former the cell size is 1.39 mm

Table 3.2: Properties of shock wave interacting with transvers flow

	a_{CF} (m/s)	$\bar{U}_{1\text{-}2}$, m/s	$\bar{M}_{1\text{-}2}$	$\pm\sigma_{1\text{-}2}$	$\bar{U}_{2\text{-}3}$, m/s	$\bar{M}_{2\text{-}3}$	$\pm\sigma_{2\text{-}3}$
Baseline	344	841	2.4	14%	625	1.8	5.8%
H_2-O_2							
5λ	535	875	1.6	5.8%	603	1.1	3.9%
10λ	535	866	1.6	6.5%	617	1.2	6.1%
15λ	535	950	1.8	20%	573	1.1	10%
20λ	535	891	1.7	17%	594	1.1	5.4%
H_2-O_2-He							
5λ	677	773	1.1	7.3%	778	1.1	8.4%
10λ	677	771	1.1	8.5%	751	1.1	7.4%
15λ	677	858	1.3	6.5%	810	1.2	7.1%
20λ	677	860	1.3	4.0%	739	1.1	6.3%

[6] and for the latter the cell size is 2.12 mm [6-9]. Measurements were made for each mixture at cross-flow heights of 5λ, 10λ, 15λ, and 20λ. Average velocities were normalized by the speed of sound within the cross-flow, a_{CF}. Results are summarized in Table 3.2.

In all cases the shock wave speed decreases between the two measurement regions. Increasing wave speeds, or even a decrease in the deceleration of the shock wave front, between these two regions would indicate additional driving of the leading shock through the combustion of the reactive cross-flow and the shedding of additional pressure waves. These results indicate that for the partially confined geometry, where the transvers flow is only confined from below, a transvers flow in excess of 20λ is required to drive a shock-combustion interaction or to reinitiate a detonation wave. The increase in the standard deviation of the velocity measurements for the H_2-O_2 for cross-flow heights of 15λ and 20λ suggest statistical outliers that may be caused by the driving of the wave front by the reaction in the transvers flow in these cases.

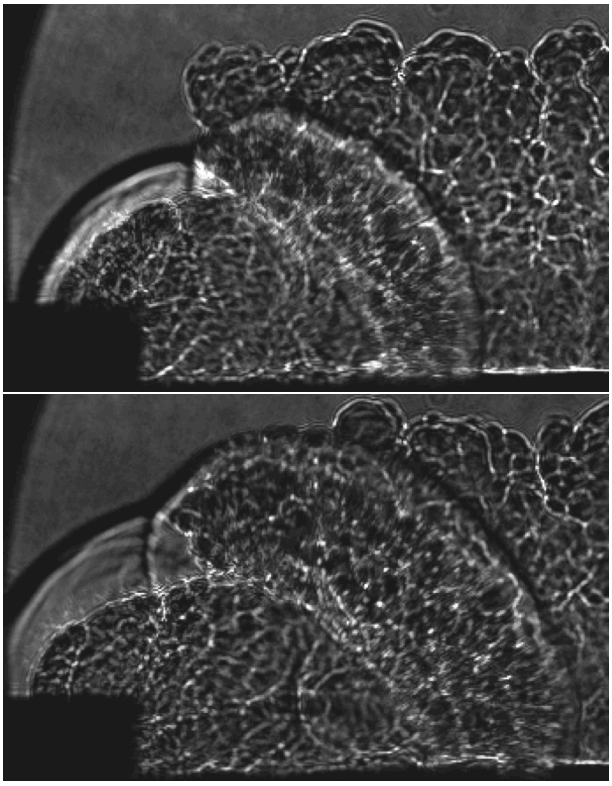

Figure 3.6. Blast wave structure propagating over transvers jets of stoichiometric hydrogen and oxygen, diluted with helium. The jets reached a height of 20 detonation cell widths, and the images were taken from two different runs.

In the absence of a sufficiently reactive material along the wave pathway, the detonation wave from the PDE decays to a blast wave upon exiting the tube. As the reactive jets were injected transversely along the y-direction, some of the cases resulted in additional interaction between the blast wave and combustion reaction. The interaction delayed the deceleration of the wave speed, and in some cases was able to maintain the wave speed.

For both the H_2-O_2 and H_2-O_2-He transvers jets, the shock front in some cases reached higher velocities than in the baseline case possibly because of the higher speed of sound in the forward direction. At the interface with the transvers flow the accelerated shock front outpaces the shock front in quiescent air, and a second shock is transmitted into the quiescent air to resolve the pressure mismatch, as seen in Fig. 3.6. It might be possible in an RDE process, such a secondary shock could produce local hot-spots, capable of re-initiating the detonation process.

Several specific observations were made from these experiments. They are listed in the following:

1. Four different cross-flow heights, 5λ, 10λ, 15λ, and 20λ, were tested for two different cross-flow compositions. In each case the blast wave forward shock decayed in intensity. The reactive cross-flow height required to sustain a blast wave in the partially confined geometry exceeds 20λ for both mixtures.

2. Pressure waves shed into a low-density region quickly attenuate in intensity. In RDEs this implies shocks reflected off of irregular annulus features are unlikely to serve as a significant thermodynamic cycle loss mechanism.

3. In cases where the shock is propagating parallel to the cross-flow/quiescent gas interface the shock front is mismatched due to discontinuous speeds of sound in the gasses. A second shock is transmitted into the material with the lower speed of sound to resolve the pressure discrepancy. The region of the flow that is twice shocked can act as a detonation ignition source for certain cross-flow mixtures.

<u>Some representative images of blast wave propagation with no side confinement</u>

- Shock wave propagation with no transvers flow

- Shock wave propagation into transvers flow of helium

- Shock wave propagation into transvers flow of H2-O2-He mixture

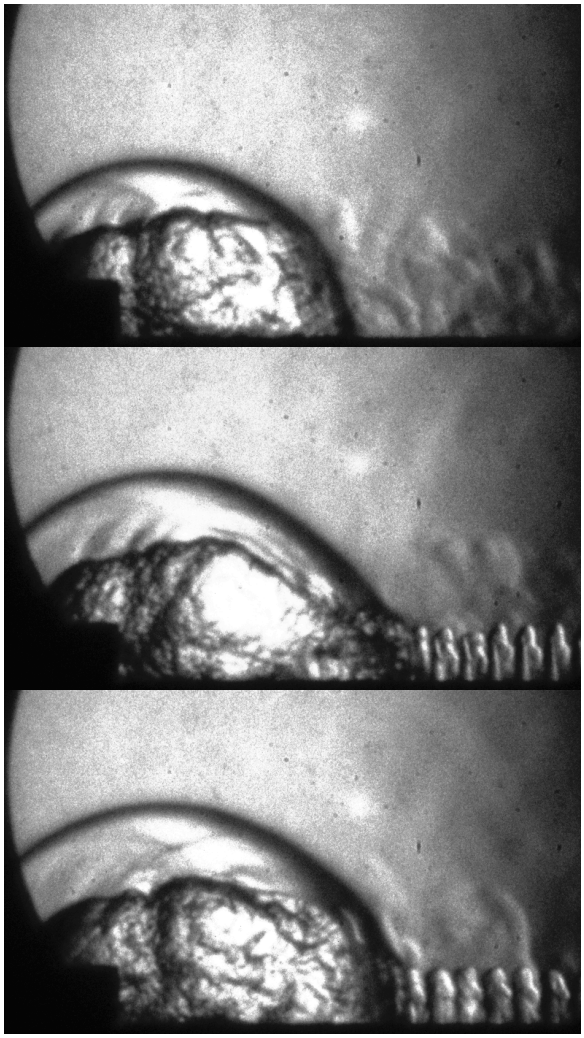

4.0 DETONATION WAVE EXPERIMENTS IN TRANSVERS FLOW CHANNEL

4.1 Objectives

The goal is to understand the RDE flow field by providing detailed experimental data on complex flow structure associated with detonation wave propagating across transverse jets of reactants. The specific objectives are to characterize the dominant flow structure of detonation waves propagating in crossflow of detonable reactants, and to study its limiting behavior of sustaining the detonation wave as a function of the crossflow height.

The approach is to experimentally characterize the flow structure under three different basic configurations including 1) no confinement - only bottom wall with pressure relief on both sides, 2) partial confinement with 90-deg angle – bottom plus one side wall with pressure relief on one side, and 3) full confinement with linear channel – bottom plus two side walls. Flow visualization experiments will be conducted while varying the crossflow jet height and reactant composition at the arrival of detonation waves.

4.2 Experimental Setup

The linear model detonation engine (LDME) serves as an "unwrapped" RDE test bed, shown in Fig. 4.1. Design of the LMDE allows for either complete optical access of the detonation channel or for non-intrusive wall-based dynamic pressure measurements through the installation of either quartz or metal walls, respectively. Attributes of both the AFRL's 6-inch RDE [3] and the NRL's numerical simulations [4] were used in the design of the LMDE.

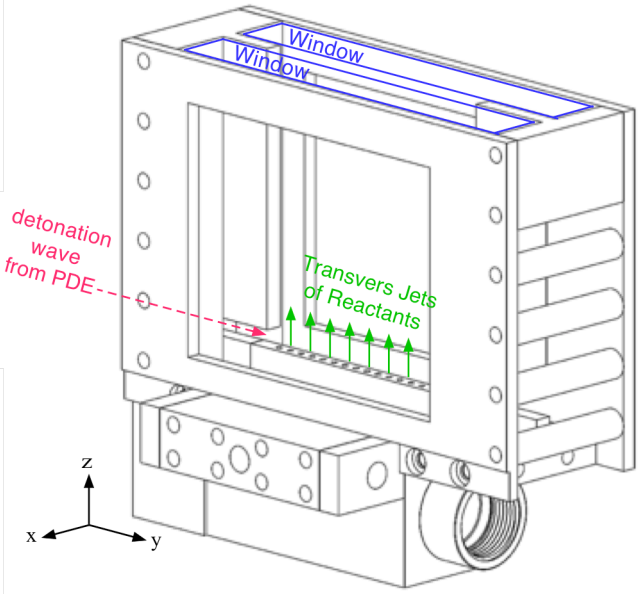

Figure 4.1. Dimetric projection of the LMDE setup. Transvers jets of reactants are established flowing in the z-direction. Detonation wave propagates in the y-direction.

Figure 4.2 illustrates the specific geometry of the LMDE injection. Gaseous hydrogen and oxygen are injected into each of the 15 pre-mixing tubes, measuring 1.125 inch in length and 0.10 inch diameter. The reactant jets are designed to be stoichiometric. Injection tubes are spaced 0.25-inch apart along the y-direction in a channel measuring 0.30 inch in width in the x-direction.

A PDE, connected to the LMDE, is used to start a detonation wave using a hydrogen-oxygen mixture. The measured wave speed in this section averaged 2420 m/s. The detonation wave then

enters the LMDE test section in the y-direction, and expands into a blast wave upon exiting the PDE tube through a 0.30-in by 0.30-in square exit.

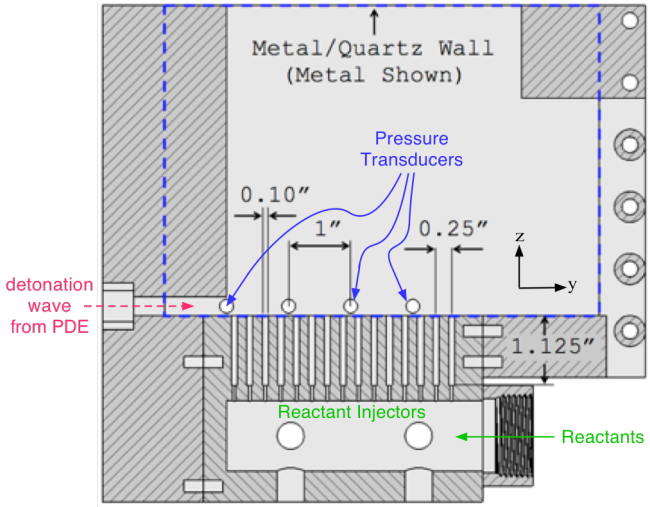

Figure 4.2. Cross-section view (y-z plane) of the LMDE. Reactants were injected at the base of the premixing tubes into the z-direction.

As before, both shadowgraph and schlieren technique have been applied to obtain flow structure images in the y-z plane. For analyzing the flow and acquiring the data, dynamic pressure transducers (PCB 113B24) were used in conjunction with a National Instruments cDAQ-9188. Two pressure transducers at the exit of the PDE determined the initial speed of the wave, while four other transducers mounted one-inch apart on the side metal wall tracked the transient propagation speed inside the test section. The PCB sensors have a range of ±1 kpsi and were sampled at 750 kHz. The measured values were sent via a TCP/IP connection to a desktop computer operating a LabView control panel.

4.3 Research Results (by Jason Burr, MS Degree Candidate)

Wave Propagation With Confinement But Without Transvers Jets

Discharge from the PDE tube was visualized without transvers flow in order to establish the baseline behavior of the blast wave structure decay in a linear channel. Figure 4.3 contains a sequence of images that are spaced approximately 20 μs apart. Inert gas used in the sequence of these tests is argon. The image acquisition was done again in a single-shot mode. The timing parameter "τ" was measured relative to when the detonation wave transited the dynamic pressure transducer which was positioned at y = -2.5 inch.

From the images in Figure 4.3, it can be observed that the shock front rapidly detaches, leaving behind it a contact surface between the shocked inert (argon) gas and the PDE exhaust. Both the contact surface and the shock front are approximately cylindrical in shape. In the earlier time steps the distance between the shock and the contact surface is small, but it quickly expands. At the later time steps, three-dimensional nature of the contact surface can be seen clearly.

Figures 4.3 (c) and (d) reveal small shocks in the region of induced flow between the shock front and the contact surface. These shocks are anchored to the injector positions and are likely the result of reflected shocks off of the lip of the injectors. For the geometry of the LMDE, the injectors partially pre-mix the fuel and oxidizer. The interface between the injectors and the channel are prime spots for re-ignition of the transversely injected reactants re-establishing a detonation wave.

A simplified model for the propagation of the blast shock front can be obtained using the cylindrical blast wave theory, which suggests the front should propagate as follows [10,11]:

$$x(t) = At^{1/2} \qquad (4.1)$$

where A is a parameter that depends on the initial energy content of the blast event. This model of a blast wave assumes a point source energy release, but in the case of the PDE discharge, the source is distributed and there's also an influx of mass, energy, and momentum behind the contact surface. Including this variation from the ideal blast wave theory, the following form is used in fitting the shock position versus time for the propagation of the shock structure:

$$x(t) = A(t - t_0)^{1/2} + B(t - t_0) \qquad (4.2)$$

where the parameters A, B and t_0 were experimentally determined from the data acquired for the case of PDE discharge into the LMDE channel without any transvers jets. Figure 4.4 shows these results along with the experimentally obtained data.

The velocity of the wave front is then determined from the time derivative of Eqn. (2). Conditions immediately behind the shock generated by the PDE blast, and along the bottom of the channel, can be approximated by the equations for a shock moving into a quiescent gas [12]:

$$M_W = \frac{u_W}{\sqrt{\gamma R T_1}} \qquad (4.3)$$

$$\frac{P_2}{P_1} = 1 + \frac{2\gamma}{\gamma+1}\left[M_W^2 - 1\right] \qquad (4.4)$$

$$\frac{T_2}{T_1} = 1 + \frac{2(\gamma-1)}{(\gamma+1)^2}\left[\gamma M_W^2 - \frac{1}{M_W^2} - (\gamma - 1)\right] \qquad (4.5)$$

$$u_2 = (u_W + u_1) - \sqrt{\gamma R T_2}\sqrt{\frac{(\gamma-1)M_W^2+2}{2\gamma M_W^2-(\gamma-1)}} \qquad (4.6)$$

where conditions at state "1" correspond to the unshocked quiescent gas, conditions at state "2" the post-shocked materials, and state "w" the shock itself. Note that using this definition $u_1 = 0$ in Equation (4.6) for the shock produced by the PDE discharge.

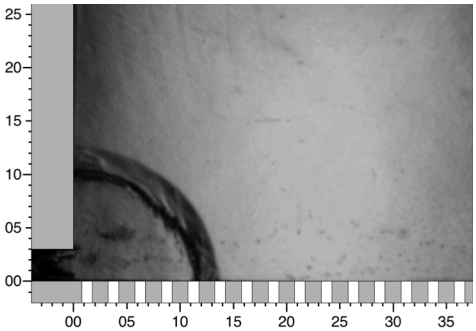

(a) τ = 41 μs

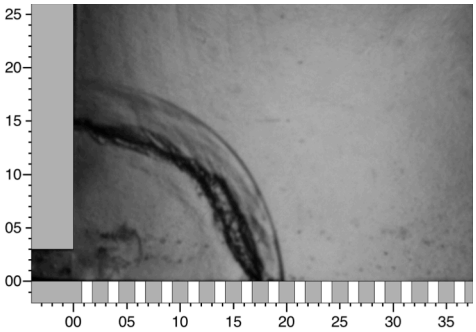

(b) τ = 61 μs

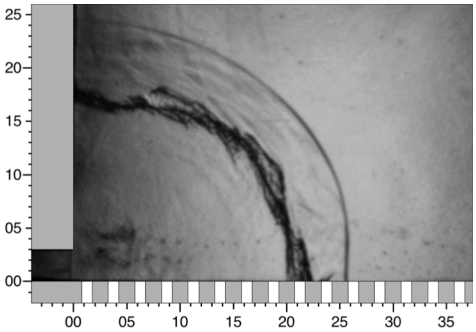

(c) τ = 81 μs

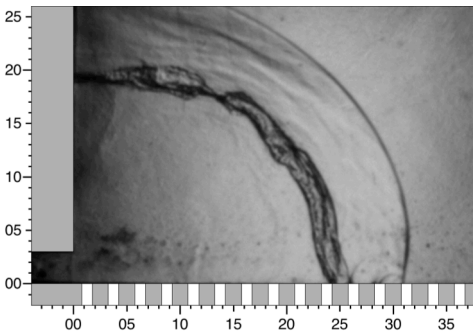

(d) τ = 103 μs

Figure 4.3. Blast wave propagation inside the LMDE channel. The physical dimensions are normalized by the injector diameter.

A reflected shock may form where injector locations exist. In general to solve for the flow properties behind the reflected shock Equations (3)-(6) are used again, but where the shock speed in Equation (4.3) is unknown. The constraint replacing this parameter is that the post-shock velocity, given by Equation (4.6) must be zero. Thus, the equations are solved iteratively for the conditions given by Equations (3)-(6).

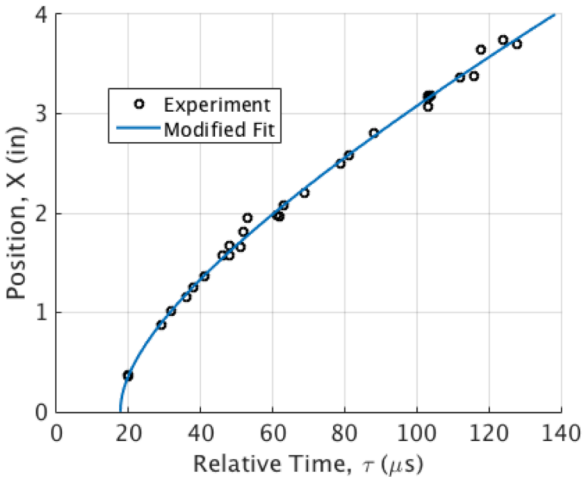

Figure 4.4. Trajectory of blast wave from PDE discharge into LMDE channel

The conditions behind the propagating shock front are calculated for both the incident shock driven by the PDE discharge and for reflected shocks along the channel bottom. Approximations to the pressure and temperature conditions are given in Figures 4.5 (a) and 4.5 (b), respectively. Stoichiometric hydrogen-oxygen mixture is assumed for these calculations with R = 693 J/kgK, γ = 1.4, T_1 = 300 K, and P_1 = 1 atm.

Figures 4.5(a) and 4.5(b) indicate some of the problems with the proposed method of approximating the conditions behind the dominant shock structures. First, the approach assumes non-reacting flow with a constant ratio of specific heats. The range of temperatures in Figure 4.5(a) that result from this analysis alone would cause variations in the heat capacities of both gases. Second, the pressures predicted by this method are extremely high. For example, a Chapman-Jouguet detonation (CJ) of a stoichiometric mixture of hydrogen and oxygen starting at 1 atm and 300 K will yield a post-detonation pressure of approximately 28 atm in a constant area duct.

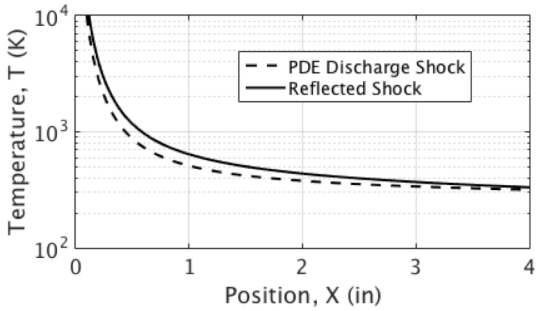

(a) Shocked Temperatures

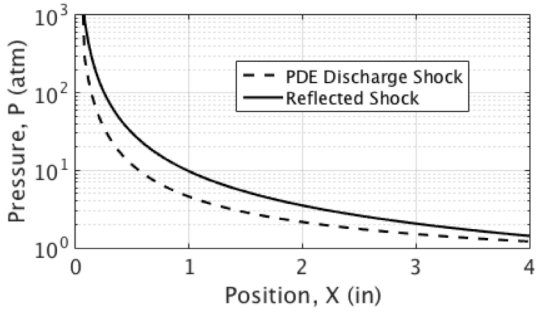

(b) Shocked Pressures

Figure 4.5. Approximated flow conditions behind incident and reflected shock structure

This is a result of the fitting scheme used on the experimental data – as *x(t)* approaches zero, then *v(t)* is driven towards infinity. An additional constraint was imposed upon the fitting scheme such that as the position nears zero the velocity instead approaches the CJ detonation velocity.

Despite the shortcomings of the fitting scheme for when *x(t)* is small, a visual inspection of Figure 4.4 indicates the fit is in

good agreement for $x(t) > 0.5$ inch, and therefore the approximated velocity should be in good agreement as well. The predicted post-shocked temperatures are still on the order of 10^3 K at this point, and the pressures on the order of 10^1 atm. In general, these conditions would be still favorable for the re-ignition of a flame or detonation structure if a stoichiometric hydrogen-oxygen mixture was present.

Wave Propagation With Transvers Jets

Transvers jets are established in the LMDE channel to simulate the flow environment of the RDE. Figure 4.6 contains a sequence of images that are spaced apart in intervals of approximately 20 μs. Inert gas used in the sequence of tests is argon. Image acquisition is in single-shot mode. The timing parameter "τ" is measured relative to when the detonation wave transits the dynamic pressure transducer positioned at y = -2.5 inch.

Timing of the transvers jet injection is controlled such that the jets reach a height of 0.80 ± 0.06 inch and are composed of a stoichiometric mixture of hydrogen and oxygen. Assuming the ideal detonation cell size of approximately 1.7 mm [13-16] for this mixture, the jet height corresponds to about 12 detonation cells.

From the images of Figure 4.6, we observe that the detonation does not directly transition from the small PDE tube into the channel, and instead collapses into a structure similar to that observed in the case where no crossflow was present in the channel at all. For some cases the detonation does not reignite and a cylindrical blast wave like flow continues. However, in a sizable number of cases the detonation reignites and structures like those observed in Figures 4.6 are observed. When the detonation does successfully reignite, expected flow structures appear - a nearly normal detonation wave, an oblique shock drug through the inert bounding gas, and an expanding contact region behind the detonation front.

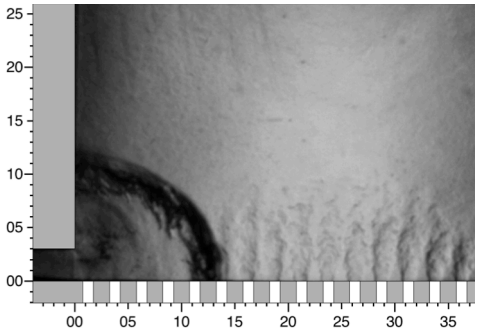

(a) τ = 40 μs

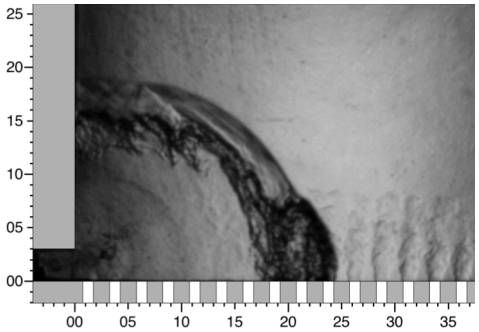

(b) τ = 60 μs

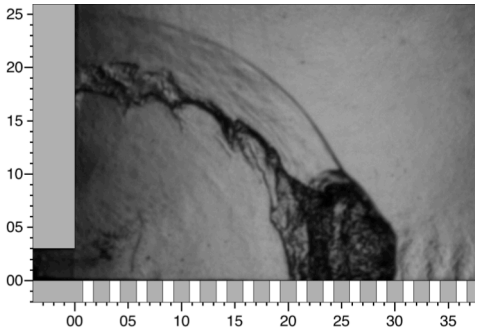

(c) τ = 80 μs

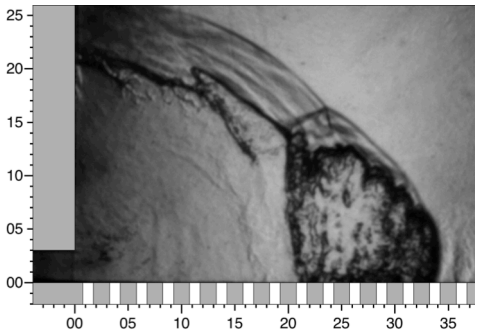

(d) τ = 100 μs

Figure 4.6. Wave propagation with transvers jets of reactive gas. The physical dimensions are normalized by the injector diameter.

In addition to these expected features, a strong shock structure propagates backwards from the detonation front along the oblique shock within the region of induced flow. This structure is caused by the sudden rise of pressure that accompanies the re-ignition of the detonation front.

Further evidence of the front taking on the form of a detonation in these cases is confirmed through dynamic pressure measurements positioned throughout the channel. Figure 4.7 shows the typical pressure traces for the sensors at various positions throughout the channel. In this figure the dashed lines represent the case without transvers jets, and the solid lines represent the case with transvers jets.

In both cases, the pressure traces for the transducers positioned at the end of the PDE, specifically those positioned at y= {-6.5", -2.5", 0"}, have nearly identical signal responses. All three signals exhibit the shape of a typical detonation transit – nearly zero measured pressure followed by a step function to a high pressure, and then a slow decay back towards zero. Note that the pressures measured by the dynamic pressure sensors are not those predicted by the Chapman-Jouguet theory – this is due to the slow response time of the sensors in comparison to the duration of the detonation transit event.

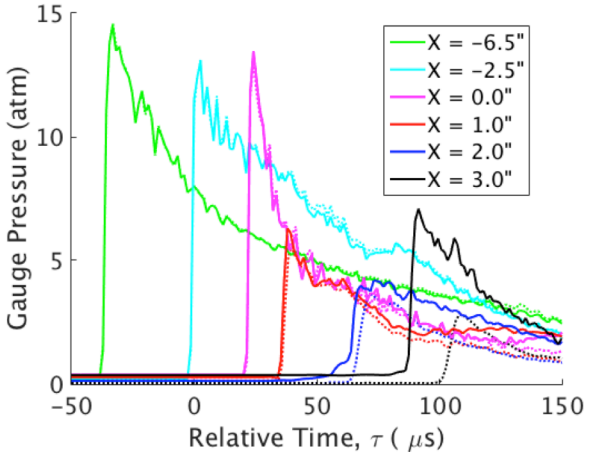

Figure 4.7. Typical dynamic pressure sensor traces for cases with (solid) and without (dashed) transvers jets.

At the first dynamic pressure sensor within the channel, y = 1.0 inch, the signals are similar in both cases. The signal qualitatively resembles a detonation transit, but the maximum pressure is half that of the preceding sensors. By the sensor positioned at y = 2.0 inch, the sharp front observed in the first four sensors has begun to spread out. When transvers jets are present the wave arrives at a marginally earlier time, indicating a slightly higher rate of transit.

The largest difference in pressure signal response occurs at the final pressure transducer, y = 3.0 inch. When no transvers jet is present the trend observed by the earlier sensors continues – the maximum pressure response continues to decrease and the "sharpness" of the wave front continues to dissipate.

When the wave passes through the transvers jets past y=2~3 inch, the pressure abruptly increases with a sharp spike indicative of a detonation event. This indicates that a detonation wave is re-initiated from a blast wave in the channel. The flow conditions at these locations can be estimated from Fig. 4.4 and the set of compressible flow equations. However, these calculations are strongly dependent on the assumption of the actual mixture ratios. Factors such as variations in the local flow composition, the degree of mixing, and possibly even turbulence intensity may be responsible for providing greatest uncertainty in the present set of data.

Some of the characteristic features of detonation waves propagating across transvers jets of reactants are illustrated in Fig. 4.8.

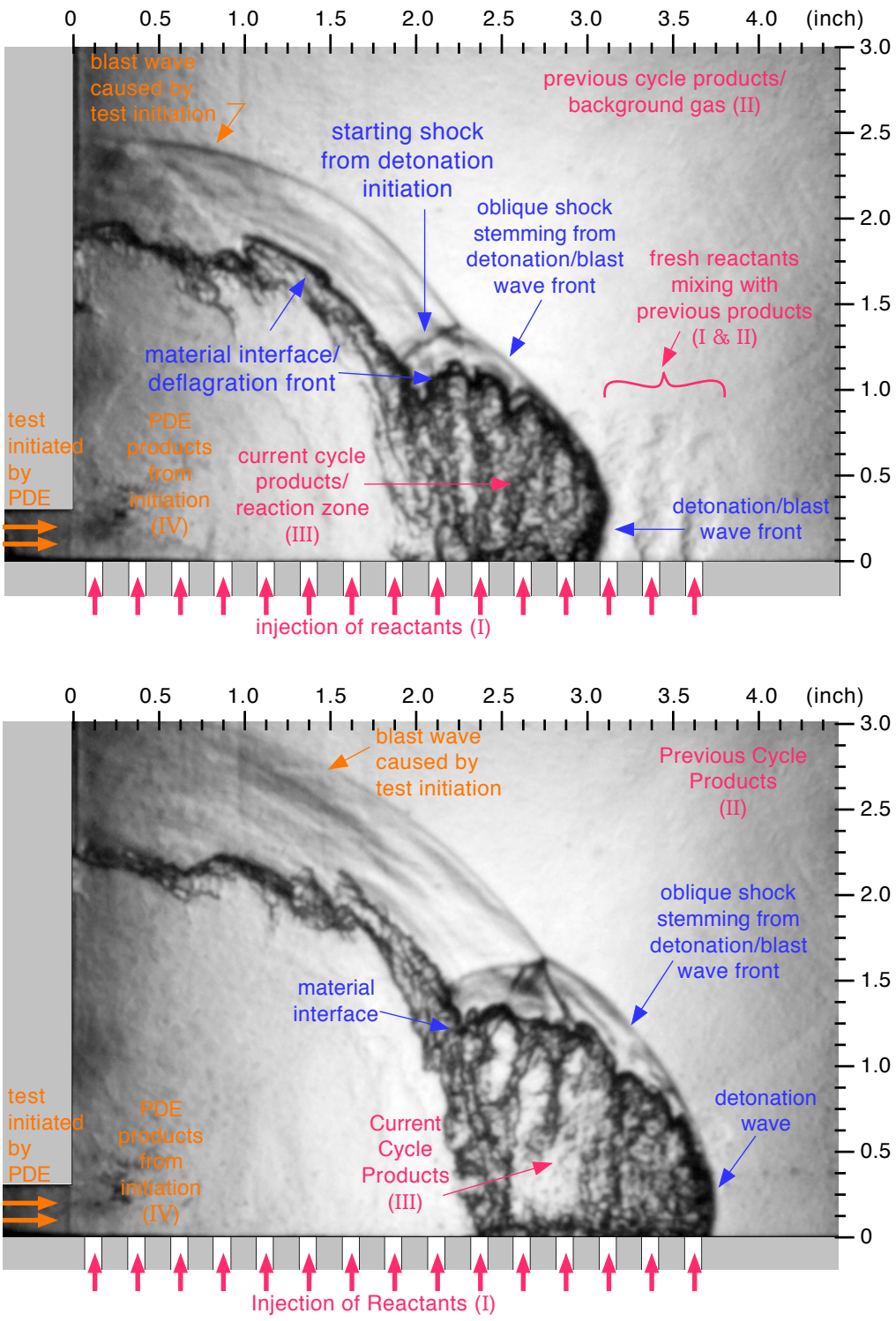

Figure 4.8. Schlieren images showing various flow structure when detonation wave passes over transvers jets of reactants

5.0 ANALYTICAL STUDY - DETONATION WAVE BOUNDED BY INERT GAS ON ONE SIDE

5.1 Objectives

This study is for complementing the experimental study outlined in the previous section. The goal is to establish a new analytical framework for estimating RDE performance parametrically and for guiding the experimental investigation. The specific objectives are to analyze the flow structure in simplified RDE flowfield, and identify important physical parameters and technical issues relevant to RDE operation.

The approach here is to model the internal flowfield of an RDE using a simple canonical configuration of detonation wave being bounded by non-reacting products from the previous cycle on the upper boundary and porous wall on the lower boundary that is acoustically closed but allows reactants inflow. This configuration would be analogous to the steady-state behavior of detonation wave propagating in crossflow of reactants at a given height.

5.2. Analytical Modeling Approach

A novel, two-dimensional, physics-based modeling approach is developed using a combination of shock-expansion theory, Chapman-Jouguet detonation theory, the Method of Characteristics (MOC), and other concepts from compressible flow theory for numerically generating an RDE flowfield. This model required the development of the first mass injection boundary condition for the two-dimensional Method of Characteristics as well as an extension of the slip line boundary condition to rotational flowfields. An improved numerical algorithm for solving the characteristic and compatibility relations along a streamline has been developed to greatly increase the accuracy over more traditional MOC algorithms in flows with large entropy gradients. A unique marching algorithm capable of marching out multiple regions concurrently along with MOC based interpolation routines have also been developed to model the unique conditions inside an RDE. Results from this model are validated against high-fidelity numerical simulations and are shown to provide similar performance estimates. The solver is used to perform a preliminary analysis of an ethylene-air RDE and several significant design parameters are identified in order to correctly size the engine and maximize performance.

Figure 5.1(a) is an idealized model of a propagating detonation bounded by an inert gas in the wave-fixed reference frame. Sommers and Morrison [1] noted that this system resembles the interaction of a shock wave incident on a free boundary and may be solved in a similar manner. Figure 5.1(b) is an extension of Fig. 5.1(a) to an RDE flowfield. The inclusion of reactants being injected in front of the detonation adds a vertical component of velocity ahead of the wave. This inclines the detonation and generates of a second expansion fan that emanates from the bottom of the detonation and turns the flow parallel to the wall. This is caused by the high-pressure detonation products preventing fresh inflow until the pressure relaxes below a certain point. Note that this model assumes no backflow of the products. Lastly, the ideal RDE flowfield model assumes there is no deflagration wave along the contact surface between the reactants and products.

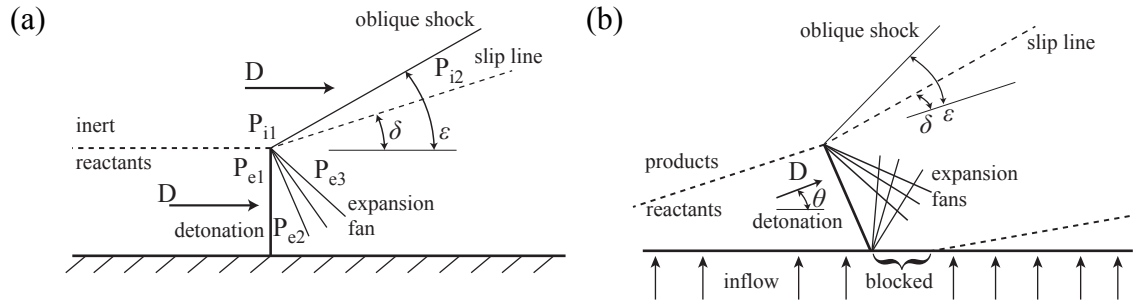

Figure 5.1. Idealized two-dimensional flowfields of detonation wave bounded by inert gas.
(a) reactants-inert gas model with zero transvers velocity, and
(b) reactants-products model with transverse injection of reactants

The simpler model of a detonation bounded by an inert gas in 5.1(a) is analyzed first to provide insights into the RDE model in 5.1(b). Following 5.1(a), if the CJ solution is provided, D and $\mathbf{P_{e2}}$ are known. The subscript **i** stands for the inert bounding gas, and the subscript **e** for the explosive mixture. Since $\mathbf{P_{e3}} = \mathbf{P_{i2}}$, there are now only three unknowns: **δ**, **ϵ**, and $\mathbf{P_{e3}}$ (or $\mathbf{P_{i2}}$). In the following analysis, $\mathbf{M_{e3}}$ is used in place of $\mathbf{P_{e3}}$, since they are related isentropically. The relationship between **δ** and **ϵ** is given by the oblique shock relation:

$$\tan\delta = 2\cot\varepsilon\left[\frac{M_{i1}^2\sin^2\varepsilon - 1}{M_{i1}^2\left(\gamma_i + \cos 2\varepsilon\right) + 2}\right] \tag{5.1}$$

Since both temperature and composition can vary across the interface, $\mathbf{M_{i1}} \neq \mathbf{M_{e1}}$. The relationship between **δ** and $\mathbf{M_{e3}}$ is given by

$$\delta = \nu(M_{e3}) - \nu(M_{e2}) \tag{5.2}$$

where $\nu(M)$ is the Prandtl-Meyer function. The pressure across the oblique shock is given by

$$\frac{P_{i2}}{P_{i1}} = 1 + \frac{2\gamma_i}{\gamma_i + 1}\left(M_{i1}^2\sin^2\varepsilon - 1\right) \tag{5.3}$$

The pressure across the expansion wave, assuming $\gamma_{e3} = \gamma_{e2}$, is given by the isentropic relation

$$\frac{P_{e2}}{P_{e3}} = \left[\frac{1 + \frac{\gamma_{e2}-1}{2}M_{e3}^2}{1 + \frac{\gamma_{e2}-1}{2}M_{e2}^2}\right]^{\gamma_{e2}/\gamma_{e2}-1} \tag{5.4}$$

Since the pressures at the material interface are equal ($P_{i2} = P_{e3}$), the pressure ratio across the shock may be expressed as:

$$\frac{P_{i2}}{P_{i1}} = \left(\frac{P_{e1}}{P_{i1}}\right)\left(\frac{P_{e2}}{P_{e1}}\right)\left(\frac{P_{e3}}{P_{e2}}\right) \tag{5.5}$$

where $\mathbf{P_{e2}}/\mathbf{P_{e1}}$ is the pressure ratio across a detonation wave. This ratio can be assessed using a detonation model, such as equilibrium Chapman-Jouguet model. This reduces the problem to three unknowns (**δ**, **ϵ** , and $\mathbf{M_{e3}}$) in three equations (Eqns. 5.1, 5.2, and 5.5). These equations may then be solved simultaneously using a nonlinear equation solver.

5.3 Research Results (by Robert Fievisohn, Ph.D. Candidate)

This model has been compared to traditional CFD methods and agrees quite well for a majority of RDE operating conditions. By solving in the wave-fixed frame, the computation time is drastically reduced which allows for large parametric studies to be accomplished in a reasonably short time frame. An example of a solution given by the MOC model is shown in Fig. 5.2 and a two-wave solution is shown in Fig. 5.3.

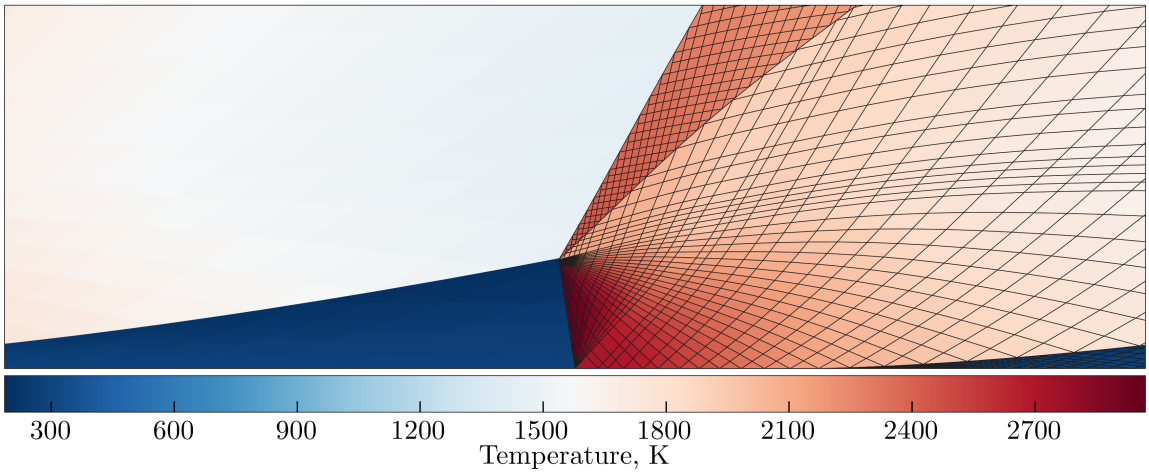

Figure 5.2. Temperature contour for unwrapped RDE one-wave solution.
P_0=10atm, T_0=300K, C=47.88cm, W=1.27cm. H=15.24cm, A_t/A_w=0.3, ϕ=1

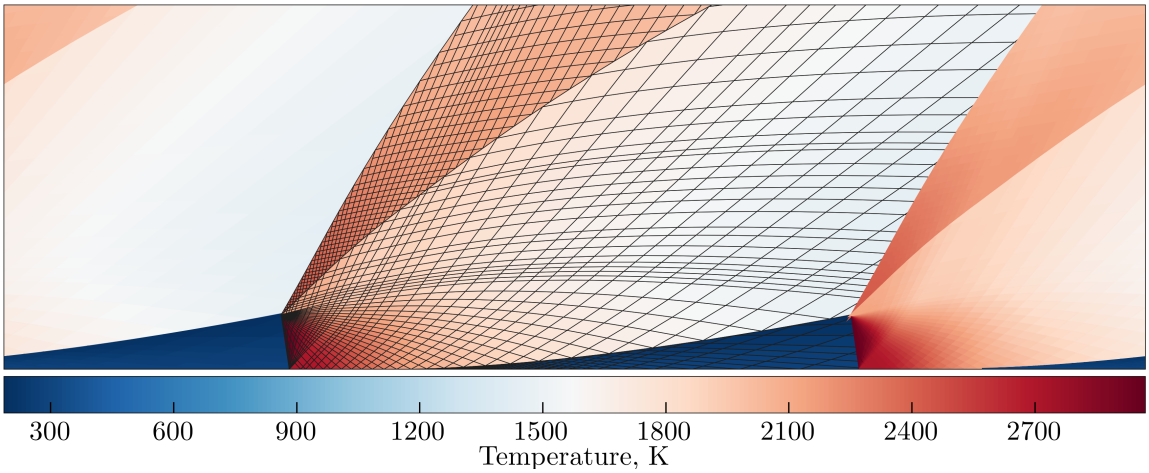

Figure 5.3. Temperature contour for unwrapped RDE two-wave solution.
P_0=10atm, T_0=300K, C=47.88cm, W=1.27cm. H=15.24cm, A_t/A_w=0.3, ϕ=1

Variations in RDE geometry, equivalence ratio, plenum conditions, and the number of detonation waves in the annulus were studied to determine their effects on a number of dependent variables. The quantities of interest were the specific impulse, thrust, mass flow rate, the average pressure ahead of the detonation wave, the length of the detonation, and the observed detonation velocity. The detonation length is dependent upon the axial height and inclination

angle. The observed detonation velocity is the velocity that would be measured in the laboratory reference frame. This takes into account the detonation inclination and transvers flow.

Effect of RDE Geometry

It was found that channel height had very little effect on any of the dependent variables examined as seen in Fig. 5.4. The only appreciable difference in any of the dependent variables was due to different values of the plenum stagnation pressure. Note that this is an ideal model that is not taking into account viscosity or heat conductivity. As channel height is increased, it is likely that these effects will become more dominate and the ideal solution will diverge from experiments.

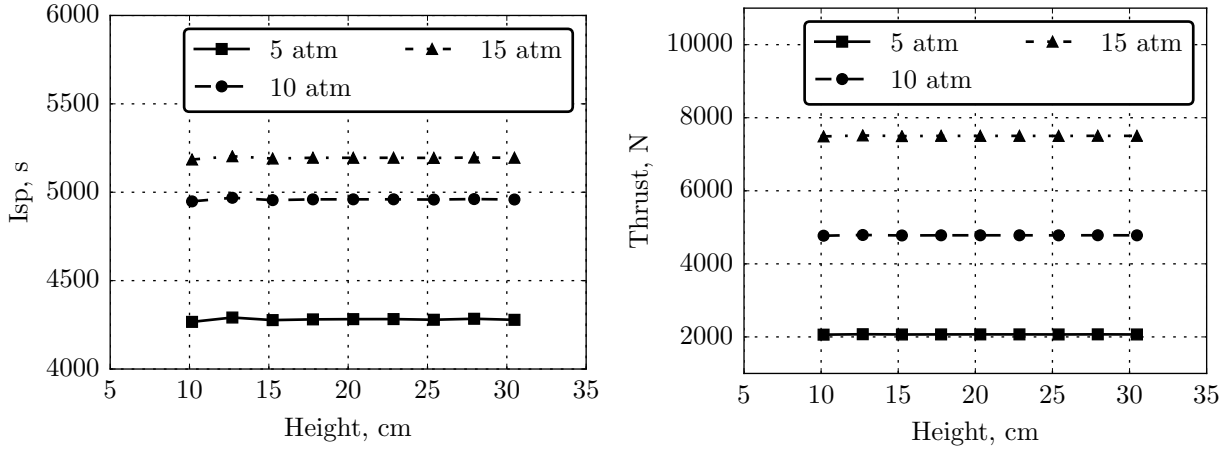

Figure 5.4. Effect of RDE channel height on performance for the selected case.

The channel width was found to only affect the mass flow rate through the RDE and thrust as seen in Fig. 5.5. Note that the injection to channel area is held constant so that as channel width increases, so does the injection area. It also appears that the thrust and mass flow scale together.

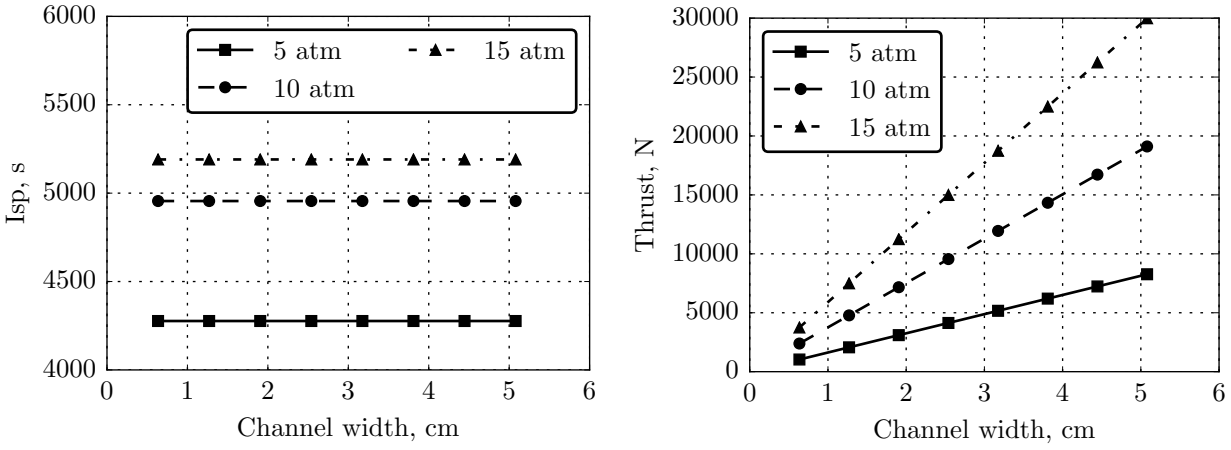

Figure 5.5. Effect of RDE channel width on performance for the selected case.

Variations in the RDE circumference are given in Fig. 5.6. As the circumference increases, the mass through the RDE and the thrust produced increase. Unlike changing the channel width, the detonation length scales linearly with circumference and the differences in stagnation

pressure have only a small effect on the detonation length. The constant pressure ahead of the detonation wave was unexpected but the changes in detonation length and mass flow rate appear to work together to keep it constant and only dependent upon the plenum stagnation pressure.

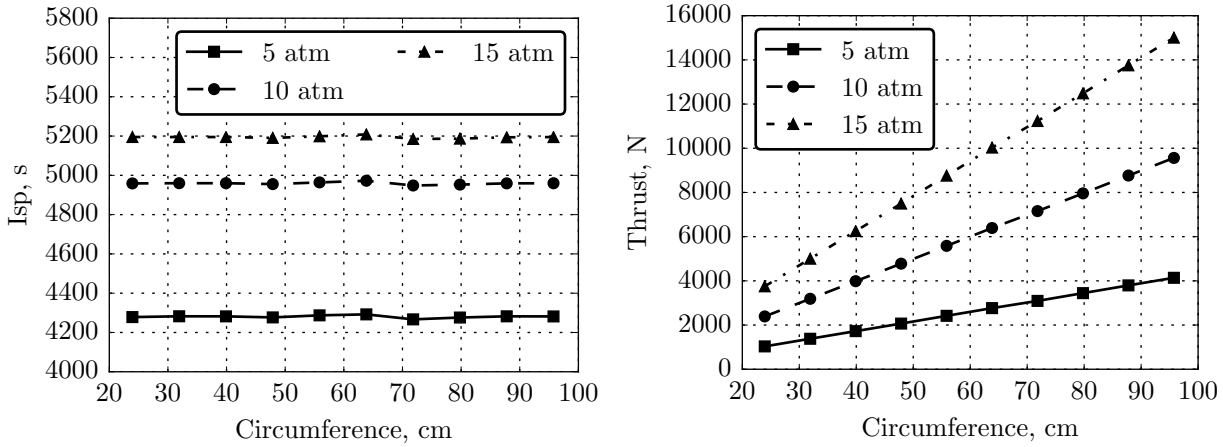

Figure 5.6. Effect of RDE circumference on performance for the selected case.

The effect of injection area to channel area ratio is seen in Fig. 5.7. It is seen that increases in the injection area lead to larger mass flows which in turn produce larger thrusts and pressures ahead of the detonation wave. Specific impulse also increases as the injection area increases with respect to the channel area. The detonation length decreases slightly and the observed detonation velocity increases slightly as the area ratio is increased. The increased pressure ahead of the detonation is expected since the larger mass flows for a given channel area require that the pressure increase. Combustion at this increased pressure also leads to the observed increases in specific impulse.

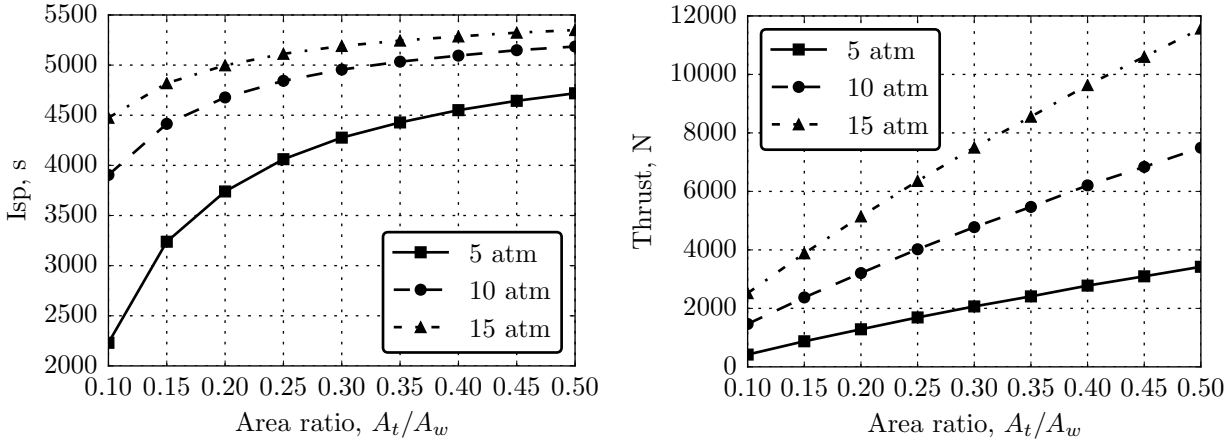

Figure 5.7. Effect of RDE injector-to-channel area ratio on performance for the selected case.

Effect of Equivalence Ratio

The effect of equivalence ratio is given in Fig. 5.8. As the mixture becomes more fuel rich, the specific impulse decreases since it is dependent on the mass flow rate of the fuel. The equivalence ratio also appears to only have a small effect on the pressure ahead of the wave, mass flow, and thrust. The detonation length hits a minimum around 1.2 and the observed

detonation velocity hits a maximum around 1.4.

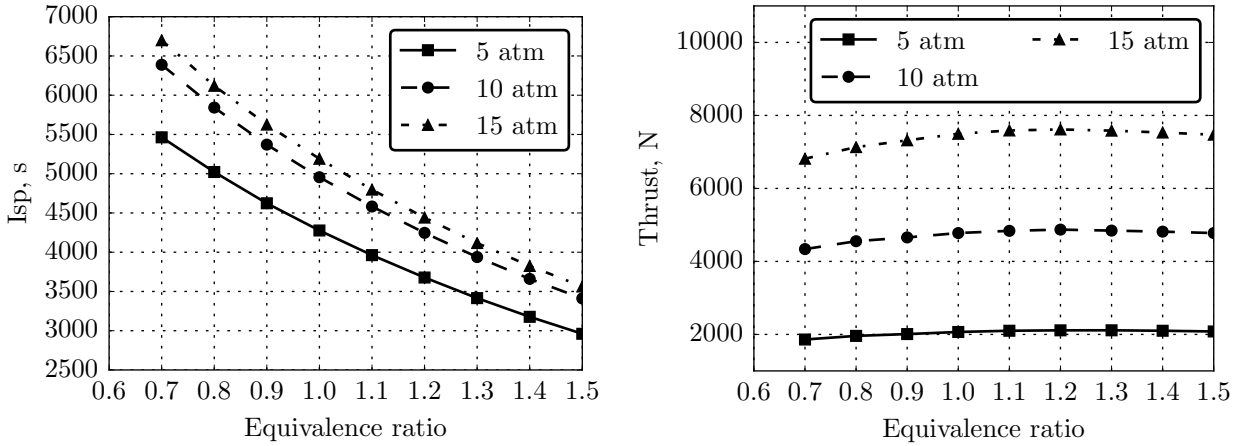

Figure 5.8. Effect of equivalence ratio on performance for the selected case.

Effect of Plenum Conditions and Multiple Waves

The effect of plenum stagnation temperature is shown in Fig. 5.9. As the temperature increases, the specific impulse, mass flow rate, and thrust decrease. This is likely due to the decrease in the density in the plenum. The pressure ahead of the wave stays relatively constant and the detonation length increases as the temperature is increased. The observed detonation velocity decreases.

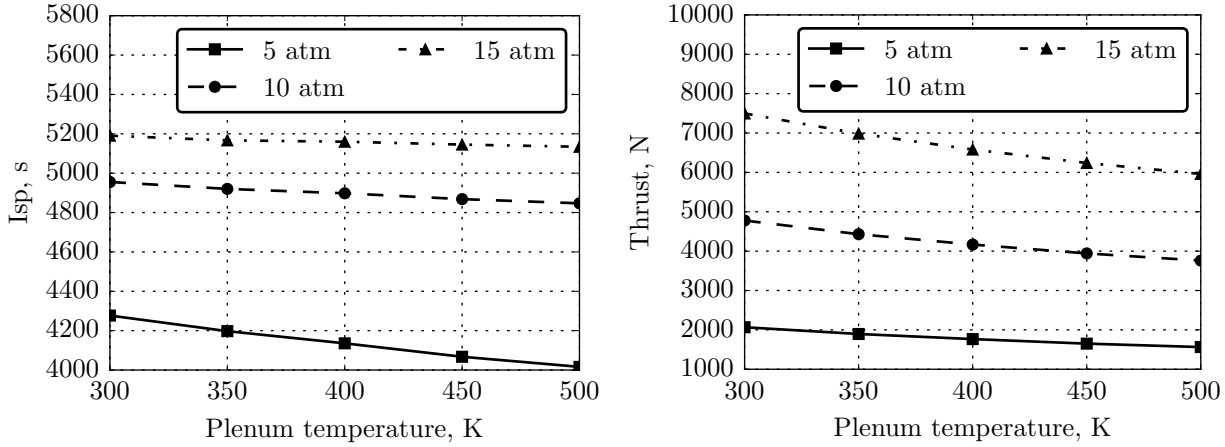

Figure 5.9. Effect of plenum stagnation temperature on performance for the selected case.

All of the figures examine the effect of plenum stagnation pressure however it is easiest to examine in Fig. 5.10 where 1- and 2-wave modes are compared as the plenum pressure is varied. As the pressure is increased, the specific impulse, pressure ahead of the detonation, mass flow, and thrust all increase. The detonation length appears to not depend on the plenum pressure. For differences in the number of waves, the only difference is in the detonation length. The number of waves appears to have no effect on any other parameter.

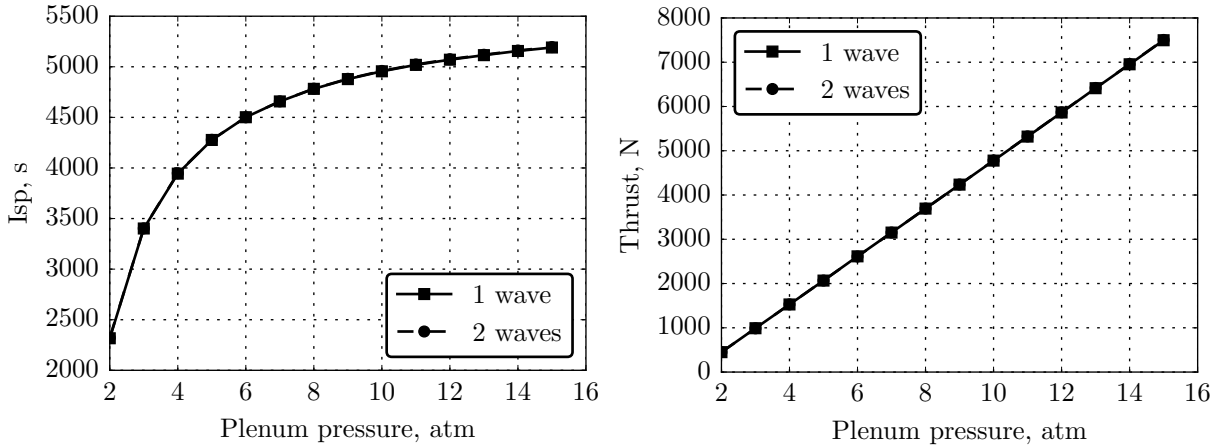

Figure 5.10. Effect of plenum stagnation pressures for 1- and 2-wave modes on performance for the selected case.

Effective Mass Flow Analysis

The goal of this parametric study is to find trends and relationships that would be useful to a researcher designing an RDE. Of particular interest is the pressure ahead of the wave. The simple detonation model used here does not take into account whether or not a detonation would be able to propagate in an actual system. There are many factors that would influence the detonability of the reactants ahead of the wave and pressure is one that may be examined by the ideal model. Examining the results of the parametric study, the pressure ahead of the wave appears to be dependent upon the plenum stagnation pressure and the injector to channel area ratio. Figure 5.11 shows the pressure ahead of the detonation wave, which is normalized by the plenum stagnation pressure, versus the injector-to-channel area ratios. All the three lines collapse onto a single line. It seems that the pressure ahead of the detonation wave is a percentage of the plenum stagnation pressure that depends on the injector to channel area ratio. In order to increase the percentage of the plenum pressure seen ahead of the detonation wave, the area ratio must be increased. Realistically, however, this can create problems with back flow due to the high pressure detonation products just behind the wave.

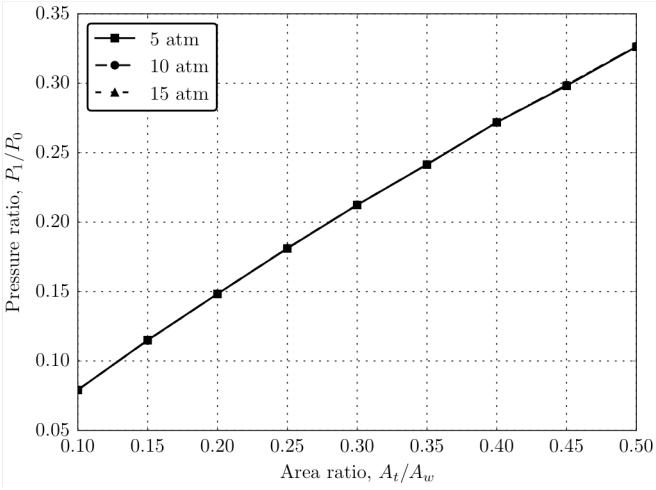

Figure 5.11. Normalized pressure ratio .vs. injector-to-channel area ratio

The mass flow through the RDE is another important variable when designing an RDE. The flow through the injectors may be blocked, unchoked, or chocked depending on the pressure at the injector face. If the mass flow is normalized by $P_0 / \sqrt{T_0}$, the three lines in Fig. 5.7c collapse onto a single line as seen in Fig. 5.12. The choked line in Fig. 5.12 represents the maximum mass

flow rate if the flow was choked along the entire injector. For the current case where the injector area increases due to an increase in the injector to channel area, the percentage of the maximum mass flow decreases. This is due to the high-pressure detonation products blocking the flow of reactants into the annulus. To represent this effect, a blockage ratio is defined as

$$B = 1 - \frac{A^*}{A_t}$$

where $\mathbf{A}^*$ is the effective throat area that is not being blocked by the high pressure detonation products.

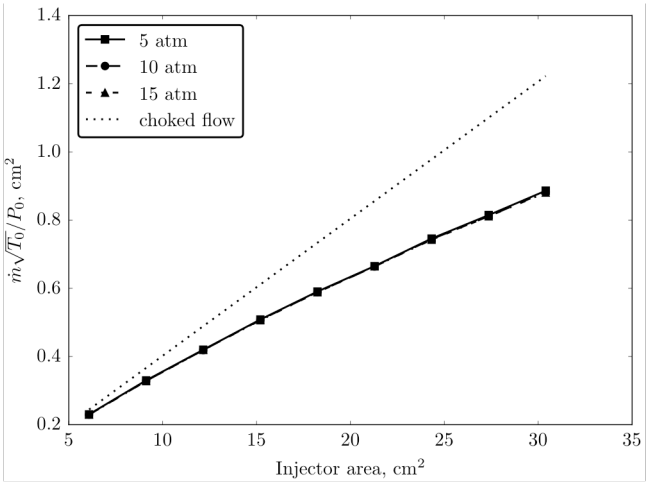

Figure 5.12. Normalized mass flow rate .vs. injector area

The mass flow in an RDE is dependent upon the channel width, channel circumference, injector to channel area ratio, plenum pressure, and plenum temperature. The width and circumference have no effect on the blockage ratio. The plenum pressure has a negligible effect on the blockage ratio. Both the plenum temperature and injector to channel area ratio have significant effects on blockage ratio with injector to channel area ratio having the largest effect.

Concluding Remarks

A parametric study for an ethylene-air RDE has been accomplished using an ideal, two-dimensional model that generates the wave-fixed, steady-state solution. The most important parameters affecting operation appears to be the injector to channel area ratio. It was found that this parameter affects the percentage of the plenum stagnation pressure that is seen ahead of the detonation wave. This can affect detonability. An RDE with higher pressures ahead of the detonation may be more likely to propagate a detonation due to the increase in detonability with increases in pressure. The injector to channel area ratio also controls the amount of blockage seen by the injector due to the high pressure detonation products. As the ratio is increased a larger percentage of the injector is effectively blocked. This has implications when sizing an RDE for a given mass flow.

It is important to note that this is an ideal model and is ignoring many important physics such as mixing, viscosity, heat conduction, and the deflagration wave that forms between the detonation products and reactants. This study is meant to be a first step towards understanding the relationship between RDE parameters and operation. The next step in this work is performing experiments and high-fidelity simulations to determine where the ideal model is applicable and where it breaks down.

REFERENCES

[1] Sommers, W. P. and Morrison, R. B., "Simulation of Condensed-Explosive Detonation Phenomena with Gases," The Physics of Fluids, Vol. 5, No. 2, Feb. 1962, pp. 241–248.

[2] Sichel, M. and Foster, J., "The ground impulse generated by a plane fuel-air explosion with side relief," Acta Astronautica,Vol. 6, No. 3, 1979, pp. 243-256.

[3] Shank J., "Development and Testing of Rotating Detonation Engine Run on Hydrogen and Air", MS Thesis, Air Force Institute of Technology, Wright-Patterson AFB, OH, 2012.

[4] Schwer D., Kailasanath K., "Feedback into Mixture Plenums in RDE", 51st AIAA Aerospace Sciences Meeting, AIAA-2012-0617, 2012.

[5] Bethe, H.A., Fuchs, K., Hirschfelder, H.O., Magee, J.L., Peierls, R.E., and von Neumann, J., "Blast Wave," LASL 2000, Los Alamos Scientific Laboratory, 1947

[6] Kaneshige M., Shepherd J.E., "Detonation database", Technical Report FM97-8, GALCIT, 1977

[7] Denisov Y.N., Troshin Y.K., "Structure of Gaseous Detonation in Tubes", Sov. Phys. Tech. Phys., 5(4), 1960, pp. 419-431.

[8] Desbordes D., "Aspects Stationnaires et Transitoires de la Detonation dans les gaz: Relation avec la Structure Cellulaire du Front", PhD thesis, Universite de Poitiers, 1990.

[9] Manzhalei V.I., Mitrofanov V.V., Subbotin V.A., "Measurement of Inhomogeneities of a Detonation Front in Gas Mixtures at Elevated Pressures", Combust. Explos. Shock Waves (USSR), 10(1), 1974, pp. 89-95.

[10] Lin, S., "Cylindrical Shock Waves Produced by Instantaneous Energy Release", Journal of Applied Physics, Vol. 25(1), 1954, pp. 54-57.

[11] Chakraborti, P.K., "An Exact Analytic Solution for a Cylindrical Blast Wave Propagating in Still Air," Proceedings of the National Institute of Sciences of India, Vol. 28(A), No. 5, 1961, pp. 683-694.

[12] Shapiro, Ascher H., *Dynamics and Thermodynamics of Compressible Fluid Flow,* Krieger Pub. Co; Reprint ed., with corrections, June 1983

[13] Kaneshige, M., and Shepherd, J.E., Detonation database, Technical Report FM97-8, GALCIT, July 1997.

[14] Yu.N. Denisov and Ya.K. Troshin, "Structure of Gaseous Detonation in Tubes," *Sov. Phys. Tech. Phys.*, 5(4), 1960, pp.419-431.

[15] D. Desbordes, "Aspects Stationnaires et Transitoires de la Detonation dans les gaz: Relation avec la Structure Cellulaire du Front," PhD thesis, Universite de Poitiers, 1990.

[16] V.I. Manzhalei, V.V. Mitrofanov, and V.A. Subbotin, "Measurement of Inhomogeneities of a Detonation Front in Gas Mixtures at Elevated Pressures," *Combust. Explos. Shock Waves (USSR)*, 10(1), 1974, pp. 89-95.

6.0 PUBLICATIONS AND PERSONNEL

6.1.Publications

[1] Fievisohn, R., and Yu, K.H., "Steady-State Analysis of Rotating Detonation Engine Flowfields with the Method of Characteristics," *Journal of Propulsion and Power*, revised/accepted (2016)

[2] Burr, J., and Yu, K.H. "Detonation Reignition within a Rotating Detonation Engine," 54th AIAA Aerospace Sciences Meeting, AIAA SciTech, San Diego, CA, AIAA-2016-1202, January (2016)

[3] Fievisohn, R., and Yu, K.H. "Parametric Study of an Ethylene-Air Rotating Detonation Engine Using an Ideal Model," 54th AIAA Aerospace Sciences Meeting, AIAA SciTech, San Diego, CA, AIAA-2016-1403, January (2016)

[4] Burr, J., and Yu, K.H. "Detonation Structure in an Unwrapped Rotating Detonation Engine," 22nd International Symposium on Air Breathing Engines, Phoenix, AZ, ISABE-2015-20237, October (2015)

[5] Burr, J., and Yu, K.H. "Shock in Reactive Crossflow under Partial Confinement," 25th International Colloquium on the Dynamics of Explosions and Reactive Systems, Reeds, UK, Paper No. 230, August (2015)

[6] Fievisohn, R., and Yu, K.H. "Method of Characteristic Analysis of Gaseous Detonations Bounded by an Inert Gas," 25th International Colloquium on the Dynamics of Explosions and Reactive Systems, Reeds, UK, Paper No. 200, August (2015)

[7] Fievisohn, R., and Yu, K.H. "Quasi-Steady Modeling of Rotating Detonation Engine Flowfields," 20th AIAA International Space Planes and Hypersonic Systems and Technologies Conference, Glasgow, UK, AIAA-2015-3616, July (2015)

[8] Fievisohn, R., and Yu, K.H. "Method of Characteristic Analysis of the Internal Flowfield in a Rotating Detonation Engine," AIAA Sci-Tech 2015, 53rd Aerospace Sciences Meeting, Kissimmee, FL, AIAA-2015-0881, January (2015)

[9] Burr, J., and Yu, K.H. "Blast Wave Propagation in Cross-Flow of Detonable Mixture," *50th AIAA/ASME/SAE/ASEE Joint Propulsion Conference*, Cleveland, OH, AIAA-2014-3984, July (2014)

6.2. Personnel

Kenneth H. Yu	Associate Professor, Department of Aerospace Engineering, University of Maryland
Jason Burr	Graduate Research Assistant, Aerospace Engineering Degree Goal: MS/Ph.D.
Robert Fievisohn	Graduate Research Assistant, Aerospace Engineering Degree Goal: Ph.D.

6.3. Degrees Awarded

Jason Burr	M.S. in Aerospace Engineering, “Shock in Reactive Crossflow under Partial Confinement”, to be conferred in May (2016)

1.

1. Report Type

Final Report

Primary Contact E-mail

Contact email if there is a problem with the report.

yu@umd.edu

Primary Contact Phone Number

Contact phone number if there is a problem with the report

3014051333

Organization / Institution name

University of Maryland

Grant/Contract Title

The full title of the funded effort.

Fundamental Structure of High-Speed Reacting Flows: Supersonic Combustion and Detonation

Grant/Contract Number

AFOSR assigned control number. It must begin with "FA9550" or "F49620" or "FA2386".

FA9550-13-1-0080

Principal Investigator Name

The full name of the principal investigator on the grant or contract.

KENNETH H. YU

Program Manager

The AFOSR Program Manager currently assigned to the award

CHIPING LI

Reporting Period Start Date

03/27/2013

Reporting Period End Date

03/31/2016

Abstract

An experimental investigation on detonation wave propagating across a row of reactant jets in a narrow channel has been performed. The principal objective of the research was to gain better understanding of the fundamental flow structure in a rotating detonation engine (RDE). A linear channel simulating an unwrapped RDE annulus was used for the investigation with an array of 15 injectors lining the inlet plane. The resulting flow structure caused by a detonation wave propagating across the array of reactant jets was examined as a function of reactant composition and flow rates. This setup served as the baseline configuration for investigating the RDE flow field without the curvature effect. The overall research effort comprised of the following technical elements: (1) blast wave propagation under partial confinement, (2) detonation wave experiments in a transverse flow channel, (3) modeling of detonation wave in transverse flow using a method of characteristics approach. The specific objectives and results of the research of each of these program elements are summarized in this report.

Distribution Statement

This is block 12 on the SF298 form.

Distribution A - Approved for Public Release

Explanation for Distribution Statement

If this is not approved for public release, please provide a short explanation. E.g., contains proprietary information.

SF298 Form

Please attach your SF298 form. A blank SF298 can be found here. Please do not password protect or secure the PDF The maximum file size for an SF298 is 50MB.

SF 298 for FA9550-13-1-0080 Yu.pdf

Upload the Report Document. File must be a PDF. Please do not password protect or secure the PDF . The maximum file size for the Report Document is 50MB.

Final Report AFOSR FA9550-13-1-0080 Yu.pdf

Upload a Report Document, if any. The maximum file size for the Report Document is 50MB.

Archival Publications (published) during reporting period:

[1] Fievisohn, R., and Yu, K.H., "Steady-State Analysis of Rotating Detonation Engine Flowfields with the Method of Characteristics," Journal of Propulsion and Power, revised/accepted (2016)

[2] Burr, J., and Yu, K.H. "Detonation Reignition within a Rotating Detonation Engine," 54th AIAA Aerospace Sciences Meeting, AIAA SciTech, San Diego, CA, AIAA-2016-1202, January (2016)

[3] Fievisohn, R., and Yu, K.H. "Parametric Study of an Ethylene-Air Rotating Detonation Engine Using an Ideal Model," 54th AIAA Aerospace Sciences Meeting, AIAA SciTech, San Diego, CA, AIAA-2016-1403, January (2016)

[4] Burr, J., and Yu, K.H. "Detonation Structure in an Unwrapped Rotating Detonation Engine," 22nd International Symposium on Air Breathing Engines, Phoenix, AZ, ISABE-2015-20237, October (2015)

[5] Burr, J., and Yu, K.H. "Shock in Reactive Crossflow under Partial Confinement," 25th International Colloquium on the Dynamics of Explosions and Reactive Systems, Reeds, UK, Paper No. 230, August (2015)

[6] Fievisohn, R., and Yu, K.H. "Method of Characteristic Analysis of Gaseous Detonations Bounded by an Inert Gas," 25th International Colloquium on the Dynamics of Explosions and Reactive Systems, Reeds, UK, Paper No. 200, August (2015)

[7] Fievisohn, R., and Yu, K.H. "Quasi-Steady Modeling of Rotating Detonation Engine Flowfields," 20th AIAA International Space Planes and Hypersonic Systems and Technologies Conference, Glasgow, UK, AIAA-2015-3616, July (2015)

[8] Fievisohn, R., and Yu, K.H. "Method of Characteristic Analysis of the Internal Flowfield in a Rotating Detonation Engine," AIAA Sci-Tech 2015, 53rd Aerospace Sciences Meeting, Kissimmee, FL, AIAA-2015-0881, January (2015)

[9] Burr, J., and Yu, K.H. "Blast Wave Propagation in Cross-Flow of Detonable Mixture," 50th AIAA/ASME/SAE/ASEE Joint Propulsion Conference, Cleveland, OH, AIAA-2014-3984, July (2014)

Changes in research objectives (if any):

Change in AFOSR Program Manager, if any:

Extensions granted or milestones slipped, if any:

AFOSR LRIR Number

LRIR Title

Reporting Period

Laboratory Task Manager

Program Officer

Research Objectives

Technical Summary

Funding Summary by Cost Category (by FY, $K)

	Starting FY	FY+1	FY+2
Salary			
Equipment/Facilities			
Supplies			
Total			

Report Document

Report Document - Text Analysis

Report Document - Text Analysis

Appendix Documents

2. Thank You

E-mail user

May 01, 2016 01:09:37 Success: Email Sent to: yu@umd.edu